Available online at www.sciencedirect.com
ScienceDirect
Polymer 48 (2007) 2659–2664
polymer
www.elsevier.com/locate/polymer

Layer-by-Layer assembly of two polyacrylate derivatives: Effect of solvent composition and side-chain structure

Qiuxia Chen [a], Ning Ma [a], Hujun Qian [b], Liyan Wang [a,*], Zhongyuan Lu [b,**]

[a] Key Laboratory of Supramolecular Structure and Materials, College of Chemistry, Jilin University, Changchun, 130012, China
[b] State Key Laboratory of Theoretical and Computational Chemistry, Institute of Theoretical Chemistry, Jilin University, Changchun 130023, China

Received 6 December 2006; received in revised form 7 February 2007; accepted 6 March 2007
Available online 12 March 2007

Abstract

We fabricated Layer-by-Layer (LbL) assemblies of poly(8-(4-carboxy-phenoxy)-octyl acrylate) (PCPOA) and poly(3-(4-pyridyl)-propyl acrylate) (PPyPA) in solvent mixtures of tetrahydrofuran (THF) and ethanol with different compositions. It was confirmed by FT-IR spectroscopy that the driving force for the assembly was mainly hydrogen bonding. Effect of solvent composition on the assembly was investigated using UV–vis spectroscopy. The amount of polymers in the film initially decreased with increase of THF content in solvent mixture, reaching a minimal value in the range between 45% and 70%, and then increased with increase of THF content. Combined with the polymer radius of gyration obtained from Dissipative Particle Dynamics simulation, we found that the adsorption amount of polymer is small when conformation of polymer is extended in a solution. We also investigated the effect of the number of methylene groups in polymer side chains on LbL assembly. When poly(2-(4-carboxy-phenoxy)-ethyl acrylate) (PCPEA) was used instead of PCPOA, we found that more polymers were adsorbed onto the substrate. In addition, we compared the normalized growth curves of both assemblies and found that the deviation of $(PCPEA/PPyPA)_n$ from linear growth was larger than that of $(PCPOA/PPyPA)_n$.

Keywords: Solvent composition; Radius of gyration; Exponential-like growth

1. Introduction

Multilayer films via Layer-by-Layer (LbL) assembling technique have attracted much attention of scientists devoting to interfacial supramolecular assemblies since 1991 [1,2]. Various materials were used to fabricate functional multilayer films, such as polyelectrolytes [3], charged dyes [4], biomacromolecules [5] and micelles [6]. Moreover, the driving force for LbL assembly has been extended from electrostatic interaction to hydrogen bond [7,8], covalent bond [9], etc. LbL technique was proved powerful and convenient for fabricating multilayer thin films with controlled architecture and tailored properties [2], promoting the development of surface molecular engineering.

Many researches aim at obtaining a multilayer film with tunable structures by adjusting some factors in the LbL assembling process since microscopic structures play a key role in impacting the property and functionality of materials. In this regard, many efforts have been made. For example, thickness of polyelectrolyte multilayer films can be adjusted by changing salt concentration, salt type, solvent quality, or deposition time [10]. For hydrogen-bonded multilayer films assembled in organic solvents, layer thickness increased gradually with increasing polymer concentration or molecular weight [11].

Recently, effect of solvent composition on LbL assembly aroused some scientists' attention. Caruso et al. studied the influence of solvent quality on the growth of polyelectrolyte multilayer films. For their selected system, they found that the thickness of multilayer films increased considerably with increasing ethanol content in the solvent mixture [12]. For

* Corresponding author. Tel.: +86 431 85168479; fax: +86 431 85193421.
** Corresponding author. Tel.: +86 431 88498017; fax: +86 431 88498026.
E-mail addresses: wangliyan@vip.sina.com (L. Wang), luzhy@jlu.edu.cn (Z. Lu).

0032-3861/$ - see front matter © 2007 Elsevier Ltd. All rights reserved.
doi:10.1016/j.polymer.2007.03.011

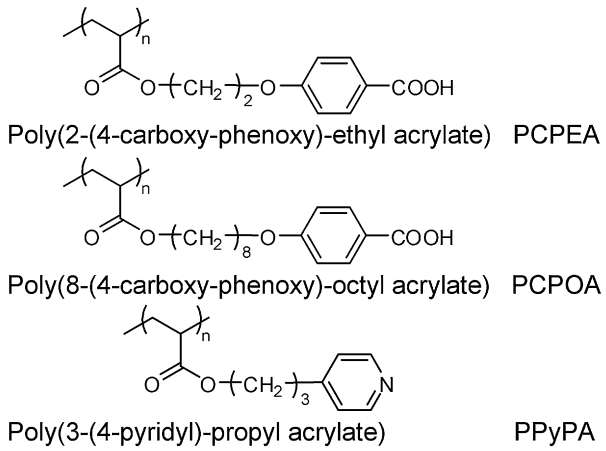

Fig. 1. Structures of the polymers.

hydrogen-bonded multilayer films, Zhang et al. found that when multilayer films composed of poly(4-vinyl pyridine) and poly(4-vinyl phenol) were prepared in an ethanol–dimethylformamide mixture, the increase of dimethylformamide content resulted in decrease of the film thickness. They inferred that this result might be due to the change in solvent polarity [13].

The conformation of polymers in the solution is related to interaction between solvent molecules and polymer chains according to polymer solution theory [14]. A few research groups discussed the effect of polymer conformation on the LbL assembly in their publications [11,15,16]. In this paper, we designed and synthesized two sorts of polyacrylate derivatives with carboxyl or pyridyl groups as shown in Fig. 1. Then LbL films were fabricated in a mixture of THF and ethanol with different compositions, and the relationship between the size of polymer coil and the assembling amount of polymers was analyzed. By normalizing the growth curves of multilayer films, the effect of polymer side chain on the exponential-like growth behavior was studied.

2. Experimental section

2.1. Materials

8-Bromo-octanol, 4-hydroxybenzoic acid methyl ester, azobisisobutyronitrile (AIBN) and 4-pyridinepropanol were bought from Aldrich. 18-Crown-6 and poly(ethyleneimine) (PEI, average molecular weight is 5×10^4) were bought from Acros. Acryloyl chloride was bought from Fluka. Potassium carbonate, potassium hydroxylate, triethyl amine and sodium hydrogen carbonate were purchased from Beijing Chemical Reagent Company. Ethanol, tetrahydrofuran (THF) and other solvents were of analytical grade. These agents were used as received if not mentioned specifically. Quartz slides and CaF_2 plates were purchased from Changchun Institute of Science and Technology.

Poly(8-(4-carboxy-phenoxy)-octyl acrylate) (PCPOA) and poly(2-(4-carboxy-phenoxy)-ethyl acrylate) (PCPEA) were synthesized using a procedure reported by Kato et al. [17]. ^{1}H NMR for PCPOA (DMSO-d_6, 500 MHz, ppm): δ 12.50 (carboxyl); 7.84, 7.01 (phenyl); 3.92 (–O–CH_2–); 1.64, 1.50, 1.23 (aliphatic). The average molecular weight was 1.07×10^4 (GPC). ^{1}H NMR for PCPEA (DMSO-d_6, 500 MHz, ppm): δ 12.59 (carboxyl); 7.83, 6.91 (phenyl); 4.20 (–O–CH_2–); 1.76, 1.59, 1.41 (aliphatic). The average molecular weight was 7.60×10^3 (GPC).

3-(4-Pyridyl)-propyl acrylate (PyPA) was synthesized by slowly mixing 4-pyridinepropanol and acryloyl chloride under low temperature of 0 °C in THF with triethyl amine. After 4 h of stirring, the mixture was concentrated and purified by silica gel column using dichloromethane as the eluent. Polymerization of PyPA was carried out in dried THF with AIBN at 60 °C under N_2 protection for about 48 h. Then the solvent was evaporated and the brown oil crude product was rinsed by cyclohexane. The residue was purified on a silica gel column using dichloromethane/methanol 15:1 as eluent. The obtained polymer (noted as PPyPA) was dried in a vacuum oven under room temperature. ^{1}H NMR for PPyPA (DMSO-d_6, 500 MHz, ppm): δ 8.48, 7.09 (pyridyl); 3.97 (–O–CH_2–); 2.50, 2.05, 1.66, 1.29 (aliphatic). The average molecular weight was around 5×10^3. (MALDI-TOF Mass Spectroscopy).

2.2. Methods

The substances synthesized in the laboratory were all characterized by ^{1}H NMR. The spectra were recorded on a Bruker Avance-500 NMR spectrometry (500 MHz) using tetramethylsilane as an internal standard. The molecular weight of PCPOA (and PCPEA) was measured by Gel Permeation Chromatography (GPC) with polystyrene as calibrated standard (Waters 410). The molecular weight of PPyPA was measured by Matrix-Assisted Laser Desorption/Ionization Time of Flight (MALDI-TOF) Mass Spectrometry (AXIMA-CFR SHIMADZU). UV–vis spectra were collected on a Perkin–Elmer Lambda 800 UV–vis spectrometry. FT-IR spectra were collected on a Bruker IFS 66V/S instrument.

2.3. Film preparation

We used quartz slide and CaF_2 plate for the UV–vis and FT-IR spectroscopies measurement, respectively. The quartz slide was modified with (3-aminopropyl)-dimethyl-methoxy-silane, resulting in an NH_2-tailored surface. CaF_2 plate was dipped in PEI aqueous solution (1 g/L) in advance.

Multilayer films were assembled in THF–ethanol mixtures with different compositions. For each film preparation, the composition of the solvent mixture used for polymer solutions was the same as the one used in the rinsing process.

The film construction process is as described below. The NH_2-tailored substrate was first immersed in PCPOA solution (0.4 g/L) for 10 min. After rinsing in the solvent for three times (1 min each time) and drying in ambient atmosphere, a PCPOA covered substrate was obtained. Then the substrate was immersed in PPyPA solution (0.3 g/L) for 10 min, resulting in a PPyPA covered substrate. By repeating the above two

steps in a cyclic fashion, we obtained multilayer films noted as $(PCPOA/PPyPA)_n$, where n is the number of bilayers. PCPEA/PPyPA multilayer films were prepared in the same way.

3. Results and discussion

The three polymers used in this paper (noted as PCPOA, PCPEA and PPyPA) were synthesized by free radical polymerization. Their chemical structures are illustrated in Fig. 1. The difference between PCPOA and PCPEA is in the number of methylene groups in side chains. There are carboxyl or pyridyl groups in the side chains of the polymers. We expected that PCPOA (or PCPEA) and PPyPA could be used to fabricate multilayer films on the basis of hydrogen bonding between carboxyl groups and pyridyl groups.

UV–vis spectroscopy is a convenient method for monitoring the assembling process of multilayer films. Fig. 2 shows the UV–vis absorption spectra of the PCPOA/PPyPA multilayer films assembled in solvent mixture with 75% THF. Since the absorbance of $\pi-\pi^*$ transition of both benzene ring and pyridine ring appears at around 256 nm, the characteristic absorption of PCPOA and PPyPA overlaps each other. Moreover, the increment of absorbance after PCPOA deposition is much greater than that for PPyPA, which is rationalized by the fact that the molar extinction coefficient of PCPOA at 256 nm is approximately 10 times larger than that of PPyPA on the basis of UV–vis spectra of polymer solutions. The gradual increase in characteristic absorbance with the number of bilayers indicates that PCPOA and PPyPA were successfully assembled into the film.

FT-IR spectroscopy was used to study the driving force of an LbL assembly. Fig. 3a shows the IR spectrum of a cast film of pure PCPOA. The broad absorption bands at around 2675 and 2555 cm^{-1} were assigned to O–H stretching vibration of carboxyl groups in an associated state. The peak at 1732 cm^{-1} was assigned to the C=O stretching vibration of an ester group and the peak at 1682 cm^{-1} was assigned to the C=O stretching vibration of a carboxyl group. Fig. 3b shows the FT-IR spectrum of a cast film of pure PPyPA. The peak at 1731 cm^{-1} was assigned to the C=O stretching vibration. The peak at 991 cm^{-1} was assigned to the in-plane breath vibration of a pyridine ring.

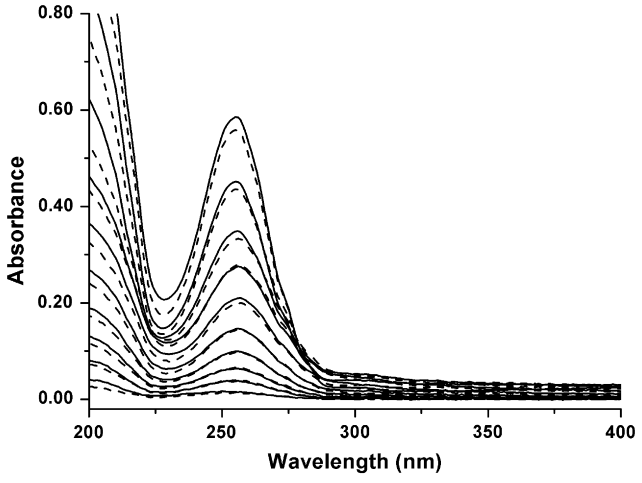

Fig. 2. UV–vis absorption spectra of the $(PCPOA/PPyPA)_n$ assembled in a solvent mixture with 75% THF. Dashed lines are the spectra of the films with PCPOA as the outmost layer, and solid lines, with PPyPA as the outmost layer.

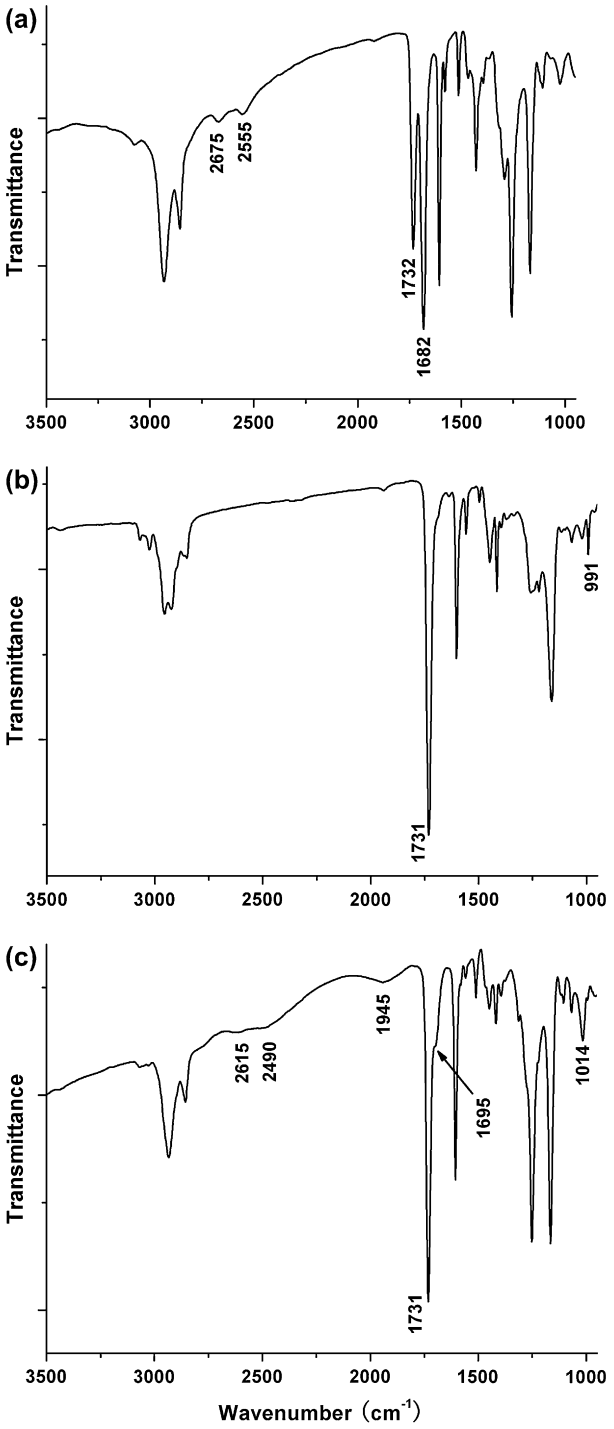

Fig. 3. FT-IR spectra of (a) a cast film of pure PCPOA, (b) a cast film of pure PPyPA, and (c) a 10-bilayer PCPOA/PPyPA film assembled in a solvent mixture with 75% THF.

Fig. 3c shows the FT-IR spectrum of a 10-bilayer film of PCPOA and PPyPA. We found that O–H vibration shifted from 2675 and 2555 cm^{-1} to 2615 and 2490 cm^{-1}. A new

broad peak appeared at 1945 cm^{-1} and it was assigned to O–H stretching vibration of a carboxyl group. This indicated that hydroxyls formed stronger hydrogen bonds in the multilayer film than in the cast film of PCPOA. The C=O vibration of carboxyl group shifted from 1682 cm^{-1} to 1695 cm^{-1}, indicating that the carbonyl of carboxyl group in the multilayer film was freed from the associated state. The in-plane breath vibration of the pyridine ring shifted from 991 cm^{-1} to 1014 cm^{-1}. This indicated that pyridyl groups formed hydrogen bonds in the multilayer film [18,19]. Thus, it is inferred that multilayer films were assembled on the basis of hydrogen bonding between carboxyl groups and pyridyl groups.

Since polymer conformation played an important role in an LbL assembly, we studied the conformation of polymers in THF–ethanol mixtures with different compositions using Dissipative Particle Dynamics (DPD) [20] simulation technique before studying the effect of solvent composition on LbL assembly. More details about DPD method can be found in Refs. [20,21]. In our simulations, a DPD bead represented a blob of an 8-(4-carboxy-phenoxy)-octyl acrylate unit, a 2-(4-carboxy-phenoxy)-ethyl acrylate unit, or a 3-(4-pyridyl)-propyl acrylate unit for PCPOA, PCPEA, or PPyPA, respectively. The mixed solvent molecules were also represented by individual DPD beads. Assuming that each polymer chain has 30 repeating units, we selected the chain length of $N = 30$ in our DPD simulations. The crucial parameter in the DPD model is the interaction parameter α_{ij} between different bead species. According to Groot and Warren [20], $\alpha_{ij} = \alpha_{ii} + 3.27\chi_{ij}$ at the reduced bead number density 3, where $\alpha_{ii} = 25$ is the interaction strength between the same kind of beads and χ_{ij} is the Flory–Huggins interaction parameter. First we calculated χ_{ij} via $\chi_{ij} = (\delta_i - \delta_j)^2 v_0 k_B^{-1} T^{-1}$, where δ is the solubility parameter (SP), v_0 is the monomer volume in DPD unit, and k_B is the Boltzmann constant. The SP of the solvent mixture was obtained by $\delta = \Phi_{Ethanol}\delta_{Ethanol} + \Phi_{THF}\delta_{THF}$, in which Φ denotes the concentration of a specific solvent. Because the length scale in the DPD is in reduced unit, the radius of gyration (R_g) in actual unit is equal to R_g in reduced unit times the monomer size, i.e., $R_g = R_g^{DPD} \times (6V/\pi)^{1/3}$, where R_g^{DPD} is obtained from DPD with reduced unit, $(6V/\pi)^{1/3}$ is the diameter of the monomer, and V is the monomer volume. All the SP and the monomer volumes of the three polymers are listed in Table 1 [22,23]. It should be noted that the persistence length is another important physical variable reflecting the size and the flexibility of macromolecules. But, accurate estimation of persistence length in a computer simulation is still under debate [24]. Moreover, both R_g and persistence length can characterize the molecule size because $R_g \sim bN^{\nu}$, where b is the persistence length and ν is the scaling parameter.

Table 1
Solubility parameters of the polymers and solvents, and the monomer volumes of different polymers

	PCPOA	PCPEA	PPyPA	Ethanol	THF
Solubility parameter $(J/cm^3)^{1/2}$	21.32	23.08	22.03	26.20	18.50
Monomer volume (nm^3)	46.2	30.2	26.9		

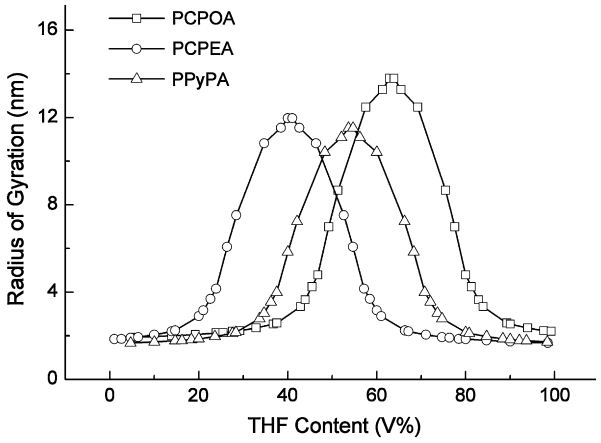

Fig. 4. Radius of gyration calculated by DPD simulation technique vs. THF content in solvent mixtures.

Therefore, in this study, we simply choose R_g to describe the macromolecule size. Fig. 4 shows R_g of the polymers as a function of THF content in the solvent mixture. As for PCPOA, R_g reached a maximal value at THF content of 63%, i.e., the polymer chain existed in the most extended conformation. The R_g curve of PPyPA peaked at 54% THF content. According to Ref. [11], polymer chains with extended conformation will form a relatively thin layer on a substrate, so that we anticipate that a thinner film will be gained if polymers are assembled in solvent mixtures with around 60% THF content.

Then we studied the effect of solvent composition on the LbL assembly by comparing multilayer films fabricated in THF–ethanol mixtures with different compositions. Fig. 5 shows the UV–vis absorbance of $(PCPOA/PPyPA)_n$ at 256 nm as a function of number of bilayers assembled from THF–ethanol mixtures with different compositions. We plotted the total absorbance of six-bilayer films as a function of THF content in the solvent mixtures, as shown by curve (a) in Fig. 6. The absorbance initially decreases with increase of the THF content, reaching a minimal value in the range between 45% and 70%, and then increases with increase of the THF content. Since the amount of polymers in the film is

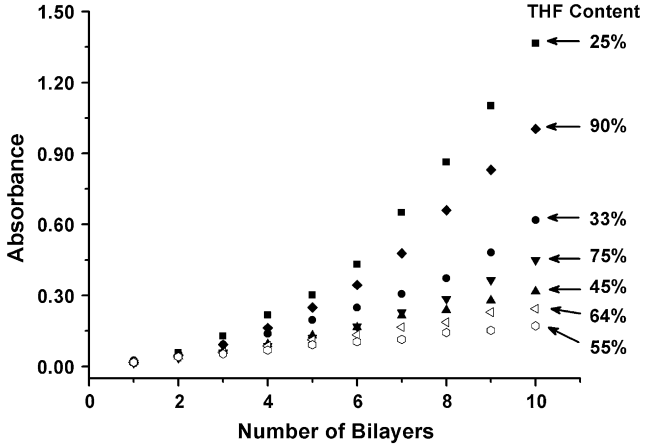

Fig. 5. UV–vis absorbance of the PCPOA/PPyPA multilayer film at 256 nm vs. the number of bilayers in several solvent mixtures.

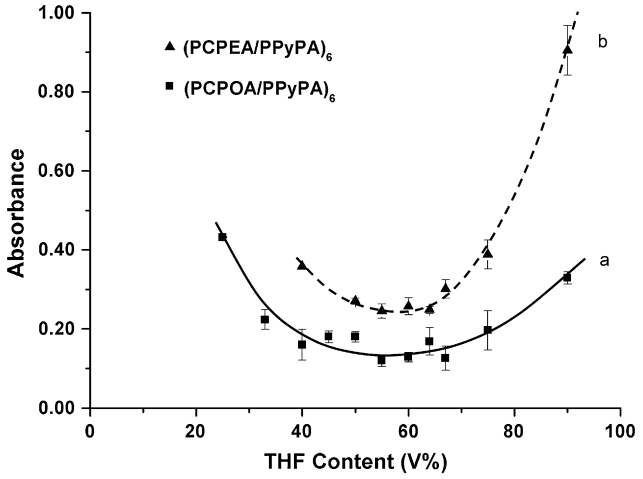

Fig. 6. Absorbance at 256 nm of $(PCPOA/PPyPA)_6$ and $(PCPEA/PPyPA)_6$ vs. THF content of the solvent mixture. Triangle marks represent $(PCPEA/PPyPA)_6$ and square marks represent $(PCPOA/PPyPA)_6$. The lines through the data points serve as a guide to the eye.

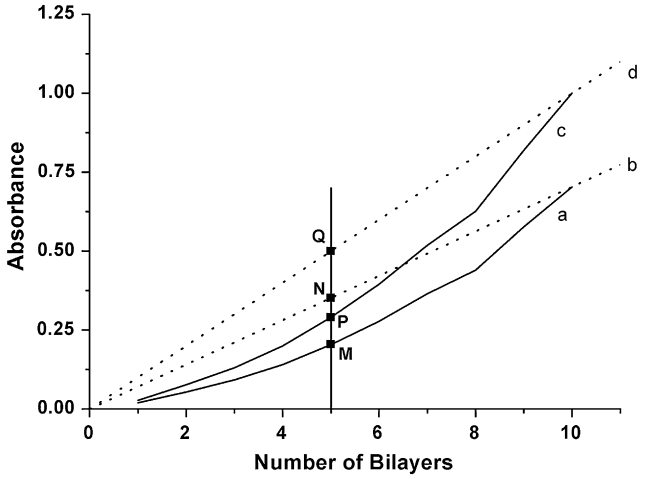

Fig. 8. Normalization process of a typical exponential growth curve: (a) is an experimental growth curve of $(PCPEA/PPyPA)_{10}$ assembled in a solvent mixture; (b) is an ideal linear growth curve; (c) and (d) were normalized experimental growth curve and normalized ideal linear growth curve, respectively.

proportional to the absorbance, curve (a) in Fig. 6 reflects the tendency of adsorption amount of polymers with the THF content. In Fig. 4, the maximal value of R_g of PCPOA and PPyPA appeared at 63% and 54% THF. Although there are various factors affecting the adsorption of polymers, the effect of polymer conformation is apparent on the adsorption amounts of polymers in our system – the adsorption amount of polymer is small when conformation of polymer is extended in a solution. Therefore, adsorption amount of polymers can be controlled by changing solvent composition. Additionally, we noticed that R_g is related to SP difference between polymers and the solvent in the simulation. Thus it is necessary to pay attention to SP difference when selecting proper solvent for an LbL assembly. Furthermore, SP needs to be considered when designing monomer structures before an LbL assembly.

PCPEA, which has two methylene groups in the side chain, was also assembled into multilayer films with PPyPA in different solvent mixtures. Curve (b) in Fig. 6 showed the total absorbance of six-bilayer film as a function of THF content. We notice that the tendency given by total absorbance of $(PCPEA/PPyPA)_6$ with the THF content is similar to that of $(PCPOA/PPyPA)_6$. However, the absorbance of $(PCPEA/PPyPA)_6$ is higher than $(PCPOA/PPyPA)_6$ at each THF content. Since the molar extinction coefficient of PCPEA is approximately equal to that of PCPOA, the amount of polymers in $(PCPEA/PPyPA)_6$ is relatively large. Detailed growth curves of $(PCPEA/PPyPA)_n$ are shown in Fig. 7. The growth of these multilayer films is typically exponential. In order to compare the nonlinearity of growth curves in Fig. 5 and 7, we normalized those curves with a process shown in Fig. 8. Curve (a) in Fig. 8 is an experimental growth curve. Curve (b) is an ideal linear growth curve, which has the same absorbance as curve (a) when the number of bilayers is equal to 10. We defined the relative deviation from linear growth as $(A_N - A_M)/A_N$, where A_M is the absorbance of point M on

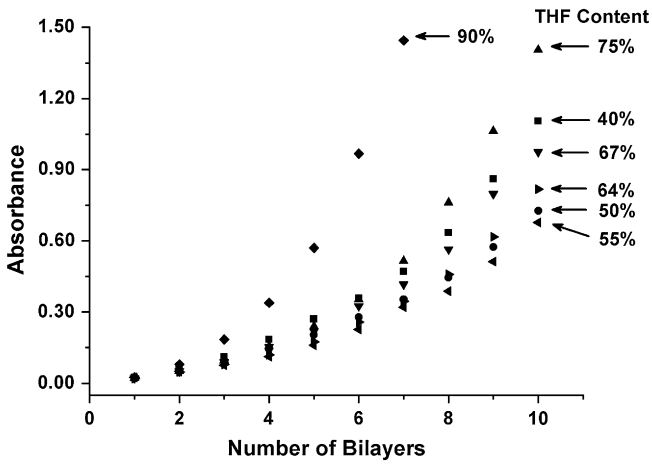

Fig. 7. UV–vis absorbance of the PCPEA/PPyPA multilayer film at 256 nm vs. the number of bilayers in several solvent mixtures.

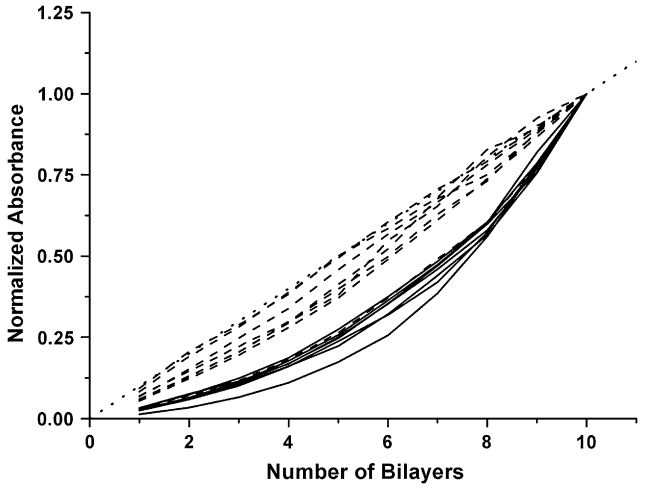

Fig. 9. Normalized absorbance vs. the number of bilayers of $(PCPOA/PPyPA)_n$ (dashed lines) and $(PCPEA/PPyPA)_n$ (solid lines) assembled in solvent mixtures with THF content from 40% to 75%.

curve (a) and A_N is the absorbance of point N on curve (b). Then, each absorbance in curve (a) and curve (b) is multiplied by a coefficient, which times the absorbance at 10 bilayers is equal to 1. In the case of curve (a), the absorbance at 10 bilayers is 0.703, so that the coefficient is $1/0.703 = 1.422$. In this way, curve (c) and curve (d) were obtained. This normalization process does not change the deviation from linear growth, because $(A_Q - A_P)/A_Q$ is equal to $(A_N - A_M)/A_N$. Fig. 9 shows the normalized growth curves from Figs. 5 and 7 with THF content in solvent between 40% and 75%. The normalization process allows us to compare conveniently the deviation of the experimental growth curves with different total absorbance, since A_Q is equal for all normalized growth curves. As shown in Fig. 9, the average deviation of $(PCPEA/PPyPA)_n$ from linear growth is larger than that of $(PCPOA/PPyPA)_n$. The difference between PCPOA and PCPEA is in the number of methylene groups in their side chains, which is responsible for the above two phenomena – difference in adsorption amount and deviation from linear growth.

4. Conclusion

In this paper, we fabricated hydrogen-bonded PCPOA/PPyPA multilayer films in THF–ethanol mixtures with different compositions. R_g of PCPOA and PPyPA in different solvent mixtures was calculated using a DPD simulation. It was found that adsorption amount of polymers was small when conformation of polymers was extended. This assembling behavior was further confirmed by the experimental result of the growth of PCPEA/PPyPA multilayer films. Therefore, based on the conformation of polymers in solution, one could anticipate the assembling behavior of polymers to some extent. Additionally, we normalized the growth curves of $(PCPOA/PPyPA)_n$ and $(PCPEA/PPyPA)_n$ in different solvent mixtures. It was found that the deviation of $(PCPEA/PPyPA)_n$ from linear growth was larger than that of $(PCPOA/PPyPA)_n$.

Acknowledgements

We thank Professor Xi Zhang (Tsinghua University, China) for his helpful discussion. This work was supported by National Natural Science Foundation of China (20674028) and National Basic Research Program (2007CB808000).

Appendix A. Supplementary data

Influence of solvent composition on the surface roughness of multilayer films can be found. The supplementary associated with this article can be found in the online version, at doi:10.1016/j.polymer.2007.03.011.

References

[1] Decher G, Hong J-D. Makromol Chem Macromol Symp 1991;46:321.
[2] Decher G, Schlenoff JB. Multilayer thin films – sequential assembly of nanocomposite materials. Weinheim: Wiley-VCH; 2003.
[3] Ferreirat M, Rubner MF. Macromolecules 1995;28:7107.
[4] Kawai T. Chem. Lett. 1993;697.
[5] Kong W, Zhang X, Gao ML, Zhou H, Li W, Shen JC. Macromol Rapid Commun 1994;15:405.
[6] Ma N, Zhang HY, Song B, Wang ZQ, Zhang X. Chem Mater 2005;17:5065.
[7] Stockton WB, Rubner MF. Macromolecules 1997;30:2717.
[8] Wang LY, Wang ZQ, Zhang X, Shen JC, Chi LF, Fuchs H. Macromol Rapid Commun 1997;18:509.
[9] Sun JQ, Wu T, Liu F, Wang ZQ, Zhang X, Shen JC. Langmuir 2000;16:4620.
[10] Dubas ST, Schlenoff JB. Macromolecules 1999;32:8153.
[11] Wang LY, Fu Y, Wang ZQ, Fan YG, Zhang X. Langmuir 1999;15:1360.
[12] Poptoshev E, Schoeler B, Caruso F. Langmuir 2004;20:829.
[13] Zhang HY, Wang ZQ, Zhang YQ, Zhang X. Langmuir 2004;20:9366.
[14] Flory PJ. Principles of polymer chemistry. Cornell University Press; 1953.
[15] Shiratori SS, Rubner MF. Macromolecules 2000;33:4213.
[16] Guyomard A, Muller G, Glinel K. Macromolecules 2005;38:5737.
[17] Kato T, Kihara H, Uryu T, Fujishima A, Frechet JMJ. Macromolecules 1992;25:6836.
[18] Odinokov SE. Spectrochim Acta 1976;32A:1355.
[19] Wang LY, Cui SX, Wang ZQ, Zhang X, Jiang M, Chi LF, et al. Langmuir 2000;16:10490.
[20] Groot R, Warren PB. J Chem Phys 1997;107:4423.
[21] Qian HJ, Lu ZY, Chen LJ, Li ZS, Sun CC. Macromolecules 2005;38:1395.
[22] Fedors RF. Polym Eng Sci 1974a;14:147.
[23] Fedors RF. Polym Eng Sci 1974b;14:472.
[24] Cifra P. Polymer 2004;45:5995.